

Example Problem CO2-6

Mineral Trapping in a Basaltic Formation

Abstract. *This problem presents a simulation of pilot-scale CO₂ injection into the flow top of the Slack Canyon #2 basalt flow in the Grande Ronde basalt formation using the STOMP-CO₂ simulator with the ECKEChem reactive transport solver. Relative amounts of CO₂ sequestration by dissolution and mineral trapping are demonstrated.*

Problem Description

Continental flood basalts represent one of the largest geologic structures on the planet but have received comparatively little attention for geologic storage of CO₂. Southeastern Washington State belongs to the Columbia Plateau Province that hosts a world-class set of continental flood basalt deposits (**Figure 1**). The U.S. Department of Energy's Big Sky Regional Carbon Sequestration Partnership has completed drilling the first continental flood basalt sequestration pilot borehole to a total depth of 4110 ft at the Boise White Paper Mill property at Wallula, Washington. Numerical simulation of CO₂ injection into basalt requires modeling complex, coupled hydrologic, chemical, and thermal processes, including multi-fluid flow and transport, partitioning of CO₂ into the aqueous phase, and chemical interactions with aqueous fluids and rock minerals. The basalt flow tops have high permeability and are good candidates for injection, whereas the intervening flow interiors have low permeability and are good confining layers. Mineral sequestration in basalts is considerably faster than in sandstone or carbonate formations (Bacon and Murphy 2011).

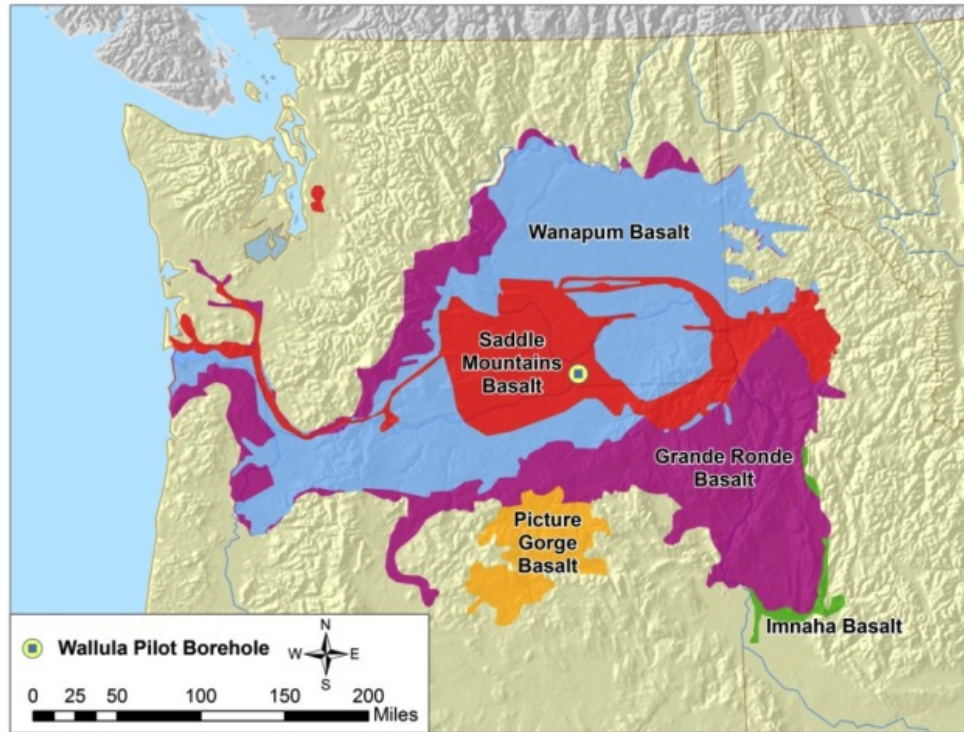


Figure 1. Surface Areal Extent of Basalt Formations of the Columbia River Basalt Group (modified from Reidel et al. 2002)

Hydraulic Properties

Hydraulic properties for the Slack Canyon #2 basalt flow top (Table 1) were determined from hydraulic test results (McGrail et al. 2011). The vertical hydraulic conductivity was assumed to be one order of magnitude lower than the horizontal hydraulic conductivity.

The unsaturated flow properties of the basalt flows have not been measured. The unsaturated flow properties assumed (White et al. 2006) are shown in Table 2. The hydraulic properties for the flow tops are similar to those of gravel.

Table 1. Hydraulic Properties of the Slack Canyon #2 basalt flow top at Wallula

| Layer | Description | Top, ft | Bottom, ft | Thickness, ft | K, cm/sec | Porosity, % |
|-------|--|---------|------------|---------------|-----------------------|-------------|
| SCFT2 | Slack Canyon #2 flow top (SCFT2) porosity zone (injection) | 2720.5 | 2768.5 | 48 | 6.53×10^{-5} | 10 |

Table 2. Brooks-Corey Function Parameters

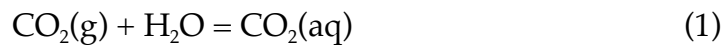
| Layer | Air-Entry Pressure, cm | λ | Residual Saturation |
|-------|------------------------|-----------|---------------------|
| SCFT2 | 54 | 4.033 | 0.01 |

A hydrostatic gradient of 0.435 psi/ft was assumed based on an observed formation pressure of 1451 psi at a measurement depth of 3568 ft below ground surface (bgs) at RRL-2 (Strait and Spane 1982). Formation temperature was assumed to be 91.23 °F at a depth of 2720.5 ft, with a geothermal gradient of - 0.147 °F/ft, based on measurements in the borehole.

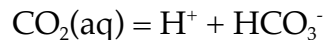
The model domain is two-dimensional with a cylindrical coordinate grid. The model domain extended from 2768.5 ft in depth to 2720.5 ft in depth (48 ft total), with a radial width of 1000 ft surrounding the injection well. Vertical grid spacing is 4 ft, while radial grid spacing is 20 ft.

Geochemical Reactions

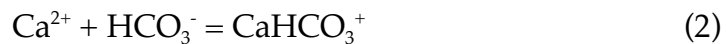
The chemical reactions caused by CO₂ injection begin with the dissolution of CO₂ in water to form weak carbonic acid:



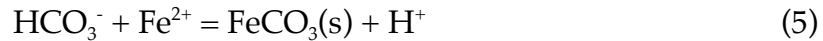
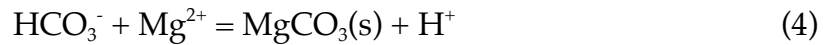
This is followed by dissociation of carbonic acid to form the bicarbonate ion:



The increased acidity causes dissolution of primary host rock minerals, which in turn causes complexing of dissolved cations with the bicarbonate ion such as



The dissolved bicarbonate species react with divalent cations to precipitate carbonates. Formation of calcium, magnesium, and ferrous carbonates are expected to be the primary mechanism by which CO₂ is immobilized (Gunter et al. 1997).



The dissolution of Columbia River Basalt under mildly acidic conditions has been assumed to be controlled by the following rate reaction:

$$r = k_{ref} A \exp \left[\frac{-E_a}{R} \left(\frac{1}{T} - \frac{1}{T_{ref}} \right) \right] \left(1 - \frac{Q}{K_{eq}} \right) 10^{(-\eta \text{ pH})}$$

where r is the reaction rate in mol s^{-1} , A is the surface area in m^2 , k is the intrinsic rate constant in $\text{mol m}^{-2} \text{s}^{-1}$, E_a is the activation energy in kJ mol^{-1} , R is the universal gas constant, T is temperature in degrees Kelvin, and η is the pH power law coefficient. The mineral composition of the basalt (Table 3), rate parameters for the primary constituents of the basalt (Table 4), and secondary minerals that may precipitate after injection of CO_2 (Table 5) are taken from laboratory experiments on Columbia River Basalt (Schaefer et al. 2010) and related batch chemistry simulations using EQ3/6 (Wolery and Jarek 2003). Kinetic data for secondary minerals were taken from published rates (Palandri and Kharaka 2004; Xu et al. 2005). Pertinent equilibrium aqueous reactions and their equilibrium coefficients were taken from the EQ3/6 version 8.0 COMP database (Wolery and Jarek 2003).

Initial conditions for aqueous species concentrations were based on groundwater sampling, from test zone 8B (McGrail et al. 2009, Appendix A). Total initial aqueous concentrations for each element are shown in Table 7.

Table 3. Mineral Composition of Columbia River Basalt

| Mineral | Volume Fraction | Specific Gravity, g cm^{-3} | Specific Surface Area, $\text{cm}^2 \text{g}^{-1}$ |
|---------------|-----------------|--------------------------------------|--|
| Plagioclase | 0.374 | 2.69 | 23 |
| Clinopyroxene | 0.191 | 3.37 | 19 |
| Glass | 0.425 | 2.65 | 22 |
| Magnetite | 0.011 | 5.2 | 12 |

Table 4. Primary Mineral Kinetic Reactions

| Reaction | log K_{eq} | k_{ref} at T_{ref} mol m ⁻² s ⁻¹ | T_{ref} °C | E_a kJ mol ⁻¹ | η |
|---|--------------|---|-----------------|-------------------------------|--------|
| Plagioclase + 6.186H ⁺ = 1.5465Al ³⁺ + 0.4535Na ⁺ + 3.093H ₂ O + 2.4535SiO ₂ + 0.5465Ca ⁺⁺ | 15.29 | 8.03×10 ⁻⁰⁸ | 60 | 42.1 | 0.626 |
| Clinopyroxene + 4H ⁺ = Ca ²⁺ + 0.25Fe ²⁺ + 0.75Mg ²⁺ + 2H ₂ O + 2SiO ₂ (aq) | 19.89 | 4.13×10 ⁻⁰⁶ | 60 | 78.0 | 0.700 |
| Glass + 0.8869H ⁺ = 0.429H ₂ O + 0.2051Al ³⁺ + 0.0378Ca ²⁺ + 0.0364Fe ²⁺ + 0.0329K ⁺ + 0.0049Mg ²⁺ + 0.0056Mn ²⁺ + 0.0693Na ⁺ + SiO ₂ (aq) + 0.007Ti(OH)4(aq) | -2.60 | 3.93×10 ⁻⁰⁸ | 100 | 30.3 | 0.318 |
| Magnetite + 6H ⁺ = 3Fe ²⁺ + 0.5O ₂ (g) + 3H ₂ O | -5.15 | 8.34×10 ⁻¹¹ | 60 | 18.6 | 0.279 |

Table 5. Secondary Mineral Kinetic Reactions

| Reaction | log K_{eq} | k_{ref} at T_{ref} mol m ⁻² s ⁻¹ | T_{ref} °C | E_a kJ mol ⁻¹ | η |
|--|--------------|---|-----------------|-------------------------------|--------|
| Anatase + 2H ₂ O = Ti(OH) ₄ (aq) | -9.65 | 4.47×10 ⁻⁰⁹ | 25 | 37.9 | 0.421 |
| Beidellite-Ca + 7.32H ⁺ + = 0.165Ca ²⁺ + 2.33Al ³⁺ + 3.67SiO ₂ (aq) | 4.65 | 1.05×10 ⁻¹¹ | 25 | 23.6 | 0.340 |
| Beidellite-K + 7.32H ⁺ + = 0.33K ⁺ + 2.33Al ³⁺ + 3.67SiO ₂ (aq) | 4.43 | 1.05×10 ⁻¹¹ | 25 | 23.6 | 0.340 |
| Beidellite-Mg + 7.32H ⁺ + = 0.165Mg ²⁺ + 2.33Al ³⁺ + 3.67SiO ₂ (aq) | 4.60 | 1.05×10 ⁻¹¹ | 25 | 23.6 | 0.340 |
| Calcite + H ⁺ = Ca ²⁺ + HCO ₃ ⁻ | 1.70 | 5.01×10 ⁻⁰¹ | 25 | 14.4 | 1.000 |
| Chalcedony = SiO ₂ (aq) | -3.56 | 5.89×10 ⁻¹³ | 25 | 74.5 | 0.000 |
| Dawsonite + 3H ⁺ = Al ³⁺ + Na ⁺ + HCO ₃ ⁻ | 3.91 | 1.00×10 ⁻⁰⁷ | 25 | 62.8 | 0.000 |
| Magnesite + H ⁺ = Mg ⁺⁺ + HCO ₃ ⁻ | 2.04 | 4.17×10 ⁻⁰⁷ | 25 | 14.4 | 1.000 |
| Rhodochrosite + H ⁺ = HCO ₃ ⁻ + Mn ²⁺ | -0.32 | 1.02×10 ⁻⁰³ | 25 | 21.0 | 0.900 |
| Siderite + H ⁺ = Fe ²⁺ + HCO ₃ ⁻ | -0.38 | 1.02×10 ⁻⁰³ | 25 | 21.0 | 0.900 |

Table 6. Equilibrium Aqueous Reactions

| Reaction | log K |
|--|---------|
| $\text{OH}^- + \text{H}^+ = \text{H}_2\text{O}$ | -13.681 |
| $\text{Al}(\text{OH})_2^+ + 2\text{H}^+ = \text{Al}^{3+} + 2\text{H}_2\text{O}$ | -10.032 |
| $\text{AlO}_2^- + 4\text{H}^+ = \text{Al}^{3+} + 2\text{H}_2\text{O}$ | -21.854 |
| $\text{AlOH}^{2+} + \text{H}^+ = \text{Al}^{3+} + \text{H}_2\text{O}$ | -4.671 |
| $\text{HCO}_3^- + \text{H}^+ = \text{CO}_2(\text{aq}) + \text{H}_2\text{O}$ | -6.297 |
| $\text{CO}_3^{2-} + 2\text{H}^+ = \text{CO}_2(\text{aq}) + \text{H}_2\text{O}$ | -16.547 |
| $\text{CaCO}_3(\text{aq}) + 2\text{H}^+ = \text{CO}_2(\text{aq}) + \text{Ca}^{2+} + \text{H}_2\text{O}$ | -13.126 |
| $\text{CaHCO}_3^+ + \text{H}^+ = \text{CO}_2(\text{aq}) + \text{Ca}^{2+} + \text{H}_2\text{O}$ | -5.236 |
| $\text{Fe}(\text{OH})_3(\text{aq}) + 2\text{H}^+ = \text{Fe}^{2+} + 0.25\text{O}_2(\text{aq}) + 2.5\text{H}_2\text{O}$ | -4.807 |
| $\text{Fe}(\text{OH})_4^- + 3\text{H}^+ = \text{Fe}^{2+} + 0.25\text{O}_2(\text{aq}) + 3.5\text{H}_2\text{O}$ | -14.407 |
| $\text{FeHCO}_3^+ + \text{H}^+ = \text{CO}_2(\text{aq}) + \text{Fe}^{2+} + \text{H}_2\text{O}$ | -3.577 |
| $\text{HAlO}_2(\text{aq}) + 3\text{H}^+ = \text{Al}^{3+} + 2\text{H}_2\text{O}$ | -15.606 |
| $\text{HSiO}_3^- + \text{H}^+ = \text{SiO}_2(\text{aq}) + \text{H}_2\text{O}$ | -9.807 |
| $\text{MgCO}_3(\text{aq}) + 2\text{H}^+ = \text{CO}_2(\text{aq}) + \text{Mg}^{++} + \text{H}_2\text{O}$ | -13.513 |
| $\text{MgHCO}_3^+ + \text{H}^+ = \text{CO}_2(\text{aq}) + \text{Mg}^{++} + \text{H}_2\text{O}$ | -5.243 |
| $\text{MnCO}_3(\text{aq}) + 2\text{H}^+ = \text{CO}_2(\text{aq}) + \text{Mn}^{++} + \text{H}_2\text{O}$ | -12.106 |
| $\text{MnHCO}_3^+ + \text{H}^+ = \text{CO}_2(\text{aq}) + \text{Mn}^{2+} + \text{H}_2\text{O}$ | -5.415 |
| $\text{MnOH}^+ + \text{H}^+ = \text{Mn}^{2+} + \text{H}_2\text{O}$ | -10.59 |
| $\text{NaHCO}_3(\text{aq}) + \text{H}^+ = \text{CO}_2(\text{aq}) + \text{Na}^+ + \text{H}_2\text{O}$ | -6.222 |
| $\text{NaHSiO}_3(\text{aq}) + \text{H}^+ = \text{Na}^+ + \text{SiO}_2(\text{aq}) + \text{H}_2\text{O}$ | -8.238 |
| $\text{OH}^- + \text{H}^+ = \text{H}_2\text{O}$ | -13.681 |
| $\text{Al}(\text{OH})_2^+ + 2\text{H}^+ = \text{Al}^{3+} + 2\text{H}_2\text{O}$ | -10.032 |
| $\text{AlO}_2^- + 4\text{H}^+ = \text{Al}^{3+} + 2\text{H}_2\text{O}$ | -21.854 |
| $\text{AlOH}^{2+} + \text{H}^+ = \text{Al}^{3+} + \text{H}_2\text{O}$ | -4.671 |

Table 7. Initial Aqueous Concentrations

| Element | Concentration, mol/L |
|---------|-------------------------|
| Al | 8.48×10^{-6} |
| Ca | 2.70×10^{-5} |
| Fe | 1.72×10^{-5} |
| K | 6.01×10^{-5} |
| Mg | 4.53×10^{-6} |
| Mn | 2.57×10^{-7} |
| Na | 4.03×10^{-3} |
| Si | 1.28×10^{-3} |
| Ti | 2.26×10^{-10} |
| pH | 9.68 |

Input File

The solution control card indicates that this problem is using STOMP-CO2 with ECKEChem and porosity changes due to mineral precipitation and dissolution.

```

~Solution Control Card
Normal,
STOMP-CO2 w/ECKEChem w/porosity,
2,
0,s,14,day,1.e-3,s,0.2,day,1.25,16,1.e-06,
14,day,10,year,0.2,day,5,day,1.15,16,1.e-06,
99999,
Variable Aqueous Diffusion,
Variable Gas Diffusion,
0,
  
```

The data from Table 3 must be entered into specific cards in the STOMP input file. The density and molecular weight of each mineral species are listed in the *Solid Species Card*. The species name must be unique and distinct from aqueous and gas species names (e.g., FeCO3(s), FeCO3_solid, solid FeCO3, FeCO3s).

```

~Solid Species Card
14,
Chalcedony,2.65,g/cm^3,60.084,kg/kmol,
Anatase,4.24,g/cm^3,79.879,kg/kmol,
Dawsonite,2.42,g/cm^3,143.995,kg/kmol,
Dolomite,2.86,g/cm^3,184.401,kg/kmol,
  
```

Calcite,2.71,g/cm³,100.087,kg/kmol,
Rhodochrosite,3.70,g/cm³,114.947,kg/kmol,
Siderite,3.94,g/cm³,115.856,kg/kmol,
Beidellite-Ca,2.83,g/cm³,366.562,kg/kmol,
Beidellite-K,2.79,g/cm³,372.852,kg/kmol,
Beidellite-Mg,2.95,g/cm³,363.960,kg/kmol,
Plagioclase,2.69,g/cm³,270.958,kg/kmol,
Clinopyroxene,3.37,g/cm³,224.436,kg/kmol,
Glass,2.65,g/cm³,60.084,kg/kmol,
Magnetite,5.20,g/cm³,231.539,kg/kmol,

The specific surface area and volume fraction of each mineral are listed in the

Lithology Card:

~Lithology Card

SCFT2,14,
Chalcedony,0.1,m²/g,0.00,
Anatase,0.1,m²/g,0.00,
Dawsonite,0.1,m²/g,0.00,
Dolomite,0.1,m²/g,0.00,
Calcite,0.1,m²/g,0.00,
Rhodochrosite,0.1,m²/g,0.00,
Siderite,0.1,m²/g,0.00,
Beidellite-Ca,0.1,m²/g,0.00,
Beidellite-K,0.1,m²/g,0.00,
Beidellite-Mg,0.1,m²/g,0.00,
Plagioclase,2.3,m²/kg,0.3366,
Clinopyroxene,1.9,m²/kg,0.1719,
Glass,2.2,m²/kg,0.3825,
Magnetite,1.2,m²/kg,0.009,

The TST rate parameters and equilibrium coefficients for each mineral from Table 4 are entered in the *Kinetic Reactions Card*, along with all aqueous species involved in the dissolution/precipitation reaction.

~Kinetic Reactions Card

14,
KnRc-20,TST,Chalcedony,1,SiO2(aq),1,1,Chalcedony,1.,
5.888e-13,mol/m² s,6.280e+4,J/mol,25.0,C,
,-3.5565,,,,
KnRc-21,TST w/ pH,Anatase,1,Ti(OH)4(aq),1.0000,1,Anatase,1.0000,
4.47e-09,mol/m² s,3.79e+4,J/mol,25.0,C,0.421,
,-9.645200,,,,
KnRc-22,TST,Dawsonite,3,Al+++ ,1.0000,Na+,1.0000,HCO3-,1.0000,2,Dawsonite,3.0000,H+,1.0000,
1.e-07,mol/m² s,6.280e+4,J/mol,25.0,C,
,3.913300,,,,
KnRc-23,TST w/ pH,Dolomite,3,Ca++,1.0000,Mg++,1.0000,HCO3-
,2.0000,2,Dolomite,1.0000,H+,2.0000,
1.74e-04,mol/m² s,5.67e+4,J/mol,25.0,C,0.5,
,2.167100,,,,
KnRc-24,TST w/ pH,Calcite,2,Ca++,1.,HCO3-,1.,2,Calcite,1.,H+,1.,
5.01e-01,mol/m² s,1.440e+4,J/mol,25.0,C,1.0,
,1.699500,,,,

```

KnRc-25,TST w/ pH,Rhodochrosite,2,HCO3-
,1.0000,Mn++,1.0000,2,Rhodochrosite,1.0000,H+,1.0000,
1.02e-03,mol/m^2 s,2.096e+4,J/mol,25.0,C,0.9,
,-0.3166000,,,,
KnRc-26,TST w/ pH,Siderite,2,Fe++,1.0000,HCO3-,1.0000,2,Siderite,1.0000,H+,1.0000,
1.02e-03,mol/m^2 s,2.096e+4,J/mol,25.0,C,0.9,
,-0.3794000,,,,
KnRc-27,TST w/ pH,Beidellite-Ca,3,Ca++,0.1650,Al+++ ,2.3300,SiO2(aq),3.6700,2,Beidellite-
Ca,1.0000,H+,7.3200,
1.05e-11,mol/m^2 s,2.36e+4,J/mol,25.0,C,0.34,
,4.651300,,,,
KnRc-28,TST w/ pH,Beidellite-K,3,K+,0.3300,Al+++ ,2.3300,SiO2(aq),3.6700,2,Beidellite-
K,1.0000,H+,7.3200,
1.05e-11,mol/m^2 s,2.36e+4,J/mol,25.0,C,0.34,
,4.434700,,,,
KnRc-29,TST w/ pH,Beidellite-Mg,3,Mg++,0.1650,Al+++ ,2.3300,SiO2(aq),3.6700,2,Beidellite-
Mg,1.0000,H+,7.3200,
1.05e-11,mol/m^2 s,2.36e+4,J/mol,25.0,C,0.34,
,4.596400,,,,
KnRc-30,TST Toward Reactants w /
pH,Plagioclase,4,Na+,0.4535,Al+++ ,1.5465,Ca++,0.5465,SiO2(aq),2.4535,2,Plagioclase,1.0,H+,6.186
,
8.03e-08,mol/m^2 s,4.21e+4,J/mol,60,C,0.626,
,15.287,,,,
KnRc-31,TST Toward Reactants w /
pH,Clinopyroxene,4,Ca++,1.0,Mg++,0.75,Fe++,0.25,SiO2(aq),2.0,2,H+,4.0,Clinopyroxene,1.0,
4.13e-06,mol/m^2 s,7.80e+4,J/mol,60,C,0.7,
,19.89,,,,
KnRc-32,TST Toward Reactants w / pH w / glass,Glass,9,SiO2(aq),5.48e-01,Al+++ ,1.90e-
01,Ca++,1.02e-01,Fe++,1.19e-01,Mg++,8.26e-02,Na+,5.81e-02,Ti(OH)4(aq),1.7e-02,K+,6.03e-
03,Mn++,1.55e-03,2,Glass,1.,H+,1.24,
7.17e-08,mol/m^2 s,3.03e+4,J/mol,100,C,0.318,
,-2.6014,,,,
KnRc-33,TST Toward Reactants w / pH,Magnetite,1,Fe++,3.,2,Magnetite,1.0,H+,6,
8.34e-11,mol/m^2 s,1.86e+4,J/mol,60,C,0.279,
,-2.4635,,,,

```

The relevant aqueous species for this simulation must be defined in the *Aqueous Species Card*. Required input includes the species name, aqueous molecular diffusion coefficient for all species, activity coefficient model option, species charge, species diameter, and species molecular weight. The species name must be unique and distinct from gas and solid species names (e.g., CO2(aq), CO2_aqueous, dissolved CO2, CO2a). Currently, the activity coefficient models include Davies, B-Dot, Pitzer and a constant coefficient option. If the constant coefficient option is chosen then the species charge, diameter, molecular weight inputs are not required. This example uses the B-dot (Helgeson 1969) activity coefficient model:

~Aqueous Species Card

31,1.e-9,cm²/s,Bdot Activity,1.0,
Al(OH)₂⁺,1.0,4.0,A,60.996,kg/kmol,
Al⁺⁺⁺,3.0,9.0,A,26.982,kg/kmol,
AlO₂⁻,1.0,4.0,A,58.980,kg/kmol,
AlOH⁺⁺,2.0,4.5,A,43.989,kg/kmol,
CO₂(aq),0.0,3.0,A,44.010,kg/kmol,
CO₃⁻⁻,2.0,5.0,A,60.009,kg/kmol,
Ca⁺⁺,2.0,6.0,A,40.078,kg/kmol,
CaCO₃(aq),0.0,0.0,A,100.087,kg/kmol,
CaHCO₃⁺,1.0,4.0,A,101.095,kg/kmol,
Fe(OH)₃(aq),0.0,3.0,A,106.869,kg/kmol,
Fe(OH)₄⁻,1.0,4.0,A,123.876,kg/kmol,
Fe⁺⁺,2.0,6.0,A,55.847,kg/kmol,
FeHCO₃⁺,1.0,4.0,A,116.864,kg/kmol,
H⁺,1.0,9.0,A,1.008,kg/kmol,
HAlO₂(aq),0.0,3.0,A,59.988,kg/kmol,
HCO₃⁻,1.0,4.0,A,61.017,kg/kmol,
HSiO₃⁻,1.0,4.0,A,77.092,kg/kmol,
K⁺,1.0,3.0,A,39.098,kg/kmol,
Mg⁺⁺,2.0,8.0,A,24.305,kg/kmol,
MgCO₃(aq),0.0,0.0,A,84.314,kg/kmol,
MgHCO₃⁺,1.0,4.0,A,85.322,kg/kmol,
Mn⁺⁺,2.0,6.0,A,54.938,kg/kmol,
MnCO₃(aq),0.0,3.0,A,114.947,kg/kmol,
MnHCO₃⁺,1.0,4.0,A,115.955,kg/kmol,
MnOH⁺,1.0,4.0,A,71.945,kg/kmol,
Na⁺,1.0,4.0,A,22.990,kg/kmol,
NaHCO₃(aq),0.0,3.0,A,84.007,kg/kmol,
NaHSiO₃(aq),0.0,0.0,A,100.081,kg/kmol,
OH⁻,1.0,3.0,A,17.007,kg/kmol,
SiO₂(aq),0.0,3.0,A,60.084,kg/kmol,
Ti(OH)₄(aq),0.0,3.0,A,115.909,kg/kmol,

Geochemical models usually assume some reactions to be in equilibrium. This assumption is often justified for some reactions, especially those involving only aqueous species. Equilibrium reactions are not zero-rate reactions but have high reaction rates and reach equilibrium quickly when transport, other reactions, or changes in physical-chemical conditions disturb it. Specifically, if the rate of a reaction is much greater than the characteristic time of the problem being solved, it should be classified as an equilibrium reaction.

Aqueous species are associated with the defined equilibrium reactions from Table 6 via the *Equilibrium Equations Card*. Required inputs include the number of species in the equilibrium equation (including the equilibrium species), species names, equilibrium reaction name, and the species exponents. The equilibrium species (indicated with the subscript *i*) is distinguished from the other species in

the equilibrium equation (indicated with the subscript j) by being the first species listed for the equilibrium equation.

~Equilibrium Equations Card

20,
 2,OH-,H+,-1.00000e+00,EqRc-1,1.0,
 3,Al(OH)2+,Al+++ ,1.00000e+00,H+,-2.00000e+00,EqRc-2,1.0,
 3,AlO2-,Al+++ ,1.00000e+00,H+,-4.00000e+00,EqRc-3,1.0,
 3,AlOH++,Al+++ ,1.00000e+00,H+,-1.00000e+00,EqRc-4,1.0,
 3,HCO3-,CO2(aq),1.00000e+00,H+,-1.00000e+00,EqRc-5,1.0,
 3,CO3--,CO2(aq),1.00000e+00,H+,-2.00000e+00,EqRc-6,1.0,
 4,CaCO3(aq),CO2(aq),1.00000e+00,Ca++,1.00000e+00,H+,-2.00000e+00,EqRc-7,1.0,
 4,CaHCO3+,CO2(aq),1.00000e+00,Ca++,1.00000e+00,H+,-1.00000e+00,EqRc-8,1.0,
 3,Fe(OH)3(aq),Fe++,1.00000e+00,H+,-2.00000e+00,EqRc-9,1.0,
 3,Fe(OH)4-,Fe++,1.00000e+00,H+,-3.00000e+00,EqRc-10,1.0,
 4,FeHCO3+,CO2(aq),1.00000e+00,Fe++,1.00000e+00,H+,-1.00000e+00,EqRc-11,1.0,
 3,HAlO2(aq),Al+++ ,1.00000e+00,H+,-3.00000e+00,EqRc-12,1.0,
 3,HSiO3-,H+,-1.00000e+00,SiO2(aq),1.00000e+00,EqRc-13,1.0,
 4,MgCO3(aq),CO2(aq),1.00000e+00,H+,-2.00000e+00,Mg++,1.00000e+00,EqRc-14,1.0,
 4,MgHCO3+,CO2(aq),1.00000e+00,H+,-1.00000e+00,Mg++,1.00000e+00,EqRc-15,1.0,
 4,MnCO3(aq),CO2(aq),1.00000e+00,H+,-2.00000e+00,Mn++,1.00000e+00,EqRc-16,1.0,
 4,MnHCO3+,CO2(aq),1.00000e+00,H+,-1.00000e+00,Mn++,1.00000e+00,EqRc-17,1.0,
 3,MnOH+,H+,-1.00000e+00,Mn+++ ,1.00000e+00,EqRc-18,1.0,
 4,NaHCO3(aq),CO2(aq),1.00000e+00,H+,-1.00000e+00,Na+,1.00000e+00,EqRc-19,1.0,
 4,NaHSiO3(aq),H+,-1.00000e+00,Na+,1.00000e+00,SiO2(aq),1.00000e+00,EqRc-20,1.0,

The *Equilibrium Reactions Card* specifies the equilibrium reaction constants to be considered in the simulation. This card is only used to specify the parameters used in the temperature dependent equations for equilibrium constants. Required inputs include the equilibrium reaction name and equation coefficients for the temperature dependent equilibrium constant. The equilibrium reaction name must be unique and distinct from kinetic reaction names (e.g., EqRc-1, E1, Equil-Reac-1, er-1).

~Equilibrium Reactions Card

20,
 EqRc-1,0.0,-13.681,0.0,0.0,0.0,1/mol,
 EqRc-2,0.0,-10.032,0.0,0.0,0.0,1/mol,
 EqRc-3,0.0,-21.854,0.0,0.0,0.0,1/mol,
 EqRc-4,0.0,-4.671,0.0,0.0,0.0,1/mol,
 EqRc-5,0.0,-6.297,0.0,0.0,0.0,1/mol,
 EqRc-6,0.0,-16.547,0.0,0.0,0.0,1/mol,
 EqRc-7,0.0,-13.126,0.0,0.0,0.0,1/mol,
 EqRc-8,0.0,-5.236,0.0,0.0,0.0,1/mol,
 EqRc-9,0.0,-4.807,0.0,0.0,0.0,1/mol,
 EqRc-10,0.0,-14.407,0.0,0.0,0.0,1/mol,
 EqRc-11,0.0,-3.577,0.0,0.0,0.0,1/mol,
 EqRc-12,0.0,-15.606,0.0,0.0,0.0,1/mol,
 EqRc-13,0.0,-9.807,0.0,0.0,0.0,1/mol,

EqRc-14,0.0,-13.513,0.0,0.0,0.0,1/mol,
 EqRc-15,0.0,-5.243,0.0,0.0,0.0,1/mol,
 EqRc-16,0.0,-12.106,0.0,0.0,0.0,1/mol,
 EqRc-17,0.0,-5.415,0.0,0.0,0.0,1/mol,
 EqRc-18,0.0,-10.590,0.0,0.0,0.0,1/mol,
 EqRc-19,0.0,-6.222,0.0,0.0,0.0,1/mol,
 EqRc-20,0.0,-8.238,0.0,0.0,0.0,1/mol,

Equation 1, which defines the dissolution of supercritical or gas phase CO₂ in brine, does not have to be explicitly defined in the Equilibrium Equations Card, as it is calculated according to Henry's Law with a correction for salinity in the equation of state module for STOMP. The aqueous CO₂ mass fraction calculated in the coupled flow and transport may be associated with the aqueous species CO₂(aq) via the *Species Link Card*. This card associates reactive species with components in the coupled flow and transport equations and defines which species name defines the system pH.

```
~Species Link Card
2,
H+,pH,
Total_CO2(aq),Aqueous CO2,
```

The final input card needed to define the reaction network is the *Conservation Equations Card*. This card specifies the conservation equations to be considered in the simulation. Conservation equations have the following general form:

$$\frac{d\sum(a_i C_i)}{dt} = 0$$

where C_i is the concentration of species i (expressed as aqueous molar concentration), and a_i is the stoichiometric coefficient of species i , and $\sum(a_i C_i)$ is the component species concentration (expressed as aqueous molar concentration). Required inputs include the component species name, number of species in the conservation equation, species names, and species stoichiometric coefficients. The component species name must begin with "Total_" followed with the species name of a reactive species in the conservation equation (e.g., Total_CO2, Total_H2CO3, Total_H+). This name specification is critical in that it links the named species with the conservation equation, making the

concentration for that species the primary unknown for the conservation equation.

~Conservation Equations Card

11,
 Total_Al+++11,Al+++1,Al(OH)2+,1,AlO2-,1,AlOH++,1,Beidellite-Ca,2.33,Beidellite-K,2.33,Beidellite-Mg,2.33,Dawsonite,1,HAlO2(aq),1,Glass,1.9e-01,Plagioclase,1.5465,
 Total_CO2(aq),16,CO2(aq),1,CO3--
 ,1,CaCO3(aq),1,CaHCO3+,1,Calcite,1,Dawsonite,1,Dolomite,2,FeHCO3+,1,HCO3-
 ,1,MgCO3(aq),1,MgHCO3+,1,MnCO3(aq),1,MnHCO3+,1,NaHCO3(aq),1,Rhodochrosite,1,Siderite
 ,1,
 Total_Ca++,9,Ca++,1,Beidellite-Ca,1.65e-
 01,CaCO3(aq),1,CaHCO3+,1,Calcite,1,Clinopyroxene,1,Dolomite,1,Glass,1.02e-
 01,Plagioclase,5.465e-01,
 Total_Fe++,8,Fe++,1,Clinopyroxene,2.5e-01,Fe(OH)3(aq),1,Fe(OH)4-
 ,1,FeHCO3+,1,Magnetite,3,Glass,1.19e-01,Siderite,1,
 Total_H+,33,H+,1,Al(OH)2+,-2,AlO2-,-4,AlOH+,-1,Beidellite-Ca,-7.32,Beidellite-K,-
 7.32,Beidellite-Mg,-7.32,CO3--,-2,CaCO3(aq),-2,CaHCO3+,-1,Calcite,-2,Clinopyroxene,-
 4,Dawsonite,-4,Dolomite,-4,Fe(OH)3(aq),-2,Fe(OH)4-,-3,FeHCO3+,-1,HAlO2(aq),-3,HCO3-,-
 1,HSiO3-,-1,Magnetite,-8,Glass,-1.24,MgCO3(aq),-2,MgHCO3+,-1,MnCO3(aq),-2,MnHCO3+,-
 1,MnOH+,-1,NaHCO3(aq),-1,NaHSiO3(aq),-1,OH-,-1,Plagioclase,-6.186,Rhodochrosite,-
 2,Siderite,-2,
 Total_K+,3,K+,1,Beidellite-K,3.3e-01,Glass,6.03e-03,
 Total_Mg++,7,Mg++,1,Beidellite-Mg,1.65e-01,Clinopyroxene,7.5e-01,Dolomite,1,Glass,8.26e-
 02,MgCO3(aq),1,MgHCO3+,1,
 Total_Mn++,6,Mn++,1,Glass,1.55e-03,MnCO3(aq),1,MnHCO3+,1,MnOH+,1,Rhodochrosite,1,
 Total_Na+,6,Na+,1,Dawsonite,1,Glass,5.81e-02,NaHCO3(aq),1,NaHSiO3(aq),1,Plagioclase,4.535e-
 01,
 Total_SiO2(aq),10,SiO2(aq),1,Beidellite-Ca,3.67,Beidellite-K,3.67,Beidellite-
 Mg,3.67,Chalcedony,1,Clinopyroxene,2,HSiO3-,1,Glass,5.48e-
 01,NaHSiO3(aq),1,Plagioclase,2.4535,
 Total_Ti(OH)4(aq),3,Ti(OH)4(aq),1,Anatase,1,Glass,1.7e-02,

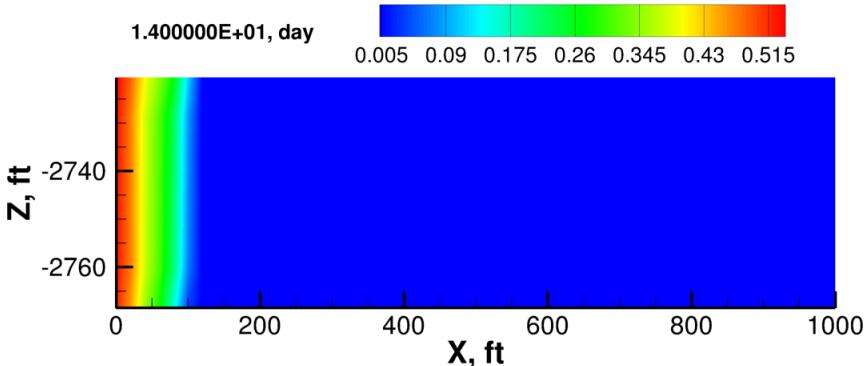
The initial conditions and Table 7 are defined in the *Initial Conditions Card*.

~Initial Conditions Card

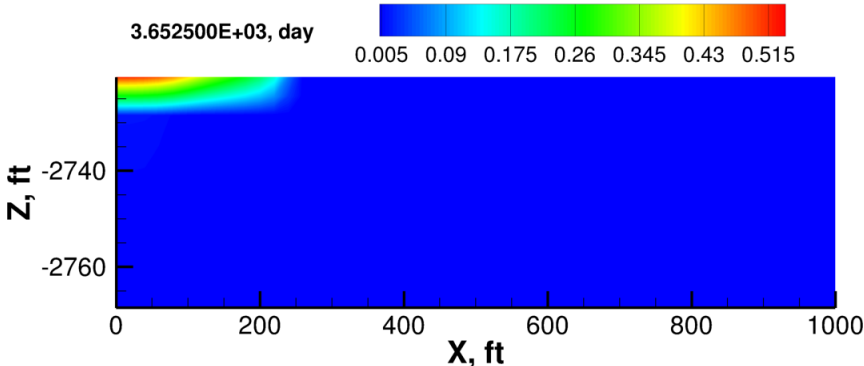
Gas Pressure,Aqueous Pressure,
 14,
 Gas Pressure,1203.863,psi,,,,,-.435,1 / ft,1,50,1,1,1,12,
 Aqueous Pressure,1203.863,psi,,,,,-.435,1 / ft,1,50,1,1,1,12,
 Temperature,91.23,F,,,,,-0.0147,1 / ft,1,50,1,1,1,12,
 Salt Mass Fraction,0.01,,,,,,1,50,1,1,1,12,
 Species Aqueous Volumetric,AlO2-,8.48e-06,mol / liter,,,,,,1,50,1,1,1,12,
 Species Aqueous Volumetric,Ca++,2.70e-05,mol / liter,,,,,,1,50,1,1,1,12,
 Species Aqueous Volumetric,Fe++,1.72e-05,mol / liter,,,,,,1,50,1,1,1,12,
 Species Aqueous Volumetric,pH,9.0,,,,,,1,50,1,1,1,12,
 Species Aqueous Volumetric,K+,6.01e-05,mol / liter,,,,,,1,50,1,1,1,12,
 Species Aqueous Volumetric,Mg++,4.53e-06,mol / liter,,,,,,1,50,1,1,1,12,
 Species Aqueous Volumetric,Mn++,2.57e-07,mol / liter,,,,,,1,50,1,1,1,12,
 Species Aqueous Volumetric,Na+,4.03e-03,mol / liter,,,,,,1,50,1,1,1,12,
 Species Aqueous Volumetric,SiO2(aq),1.28e-03,mol / liter,,,,,,1,50,1,1,1,12,
 Species Aqueous Volumetric,Ti(OH)4(aq),2.26e-10,mol / liter,,,,,,1,50,1,1,1,12,

Results

Total CO₂ injection was 1000 metric tons (MT), over a time period of 14 days. After the injection of supercritical CO₂, supercritical CO₂ rises buoyantly (Figure 2) and dissolves into the aqueous phase, up to the equilibrium solubility limit. Aqueous CO₂ dissociates into bicarbonate and carbonate ions, producing H⁺ and lowering the pH (Figure 3). The pH of the residual formation water in contact with the injected CO₂ decreases from an initial value of 9.1 to values as low as 4.1 just after injection. Over the 10-year recovery period, the pH increases slightly to a minimum value of 5.0. The lowered pH drives the dissolution of primary minerals in the basalt, producing Ca²⁺, Mg²⁺ and Fe²⁺ which combine with the aqueous CO₂ to form carbonate secondary minerals. Dolomite and calcite are the most prevalent carbonate mineral due to the release of Mg²⁺ and Ca²⁺ from the dissolution of glass, clinopyroxene and Ca²⁺ from plagioclase (Figure 4). Over time, as the injected CO₂ spreads, allowing more CO₂ to dissolve; the total amount of supercritical CO₂ decreases and amounts of dissolved and mineral CO₂ increase (Figure 5).

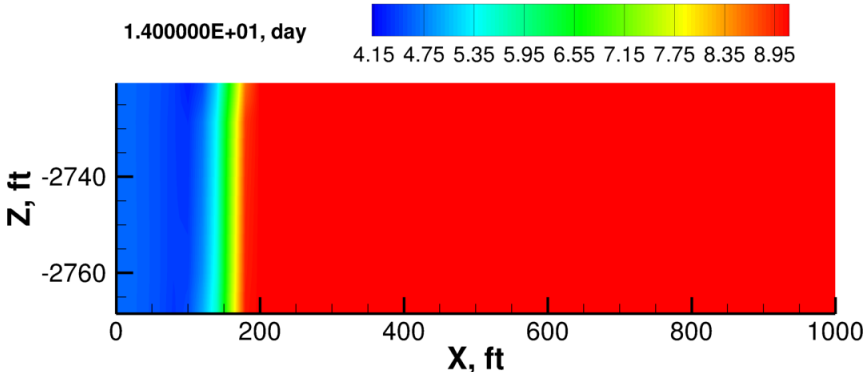


(a)

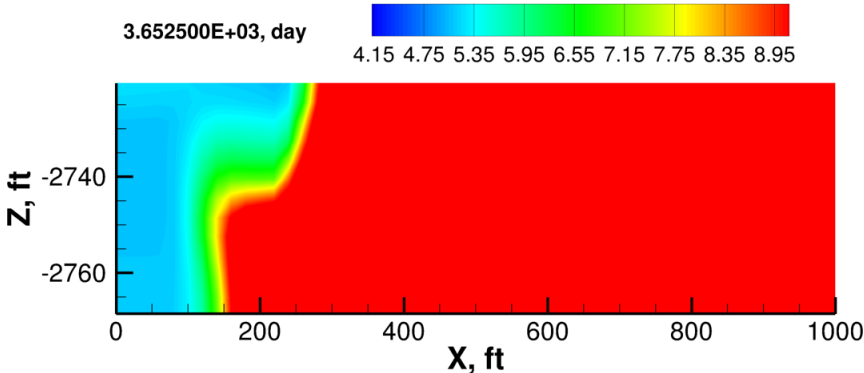


(b)

Figure 2. CO₂ Saturation (a) 14 days and (b) 10 years after 1000 MT Supercritical CO₂ Injection into the Slack Canyon #2 Flow Top



(a)



(b)

Figure 3. pH (a) 14 days and (b) 10 years after 1000 MT Supercritical CO₂ Injection into the Slack Canyon #2 Flow Top

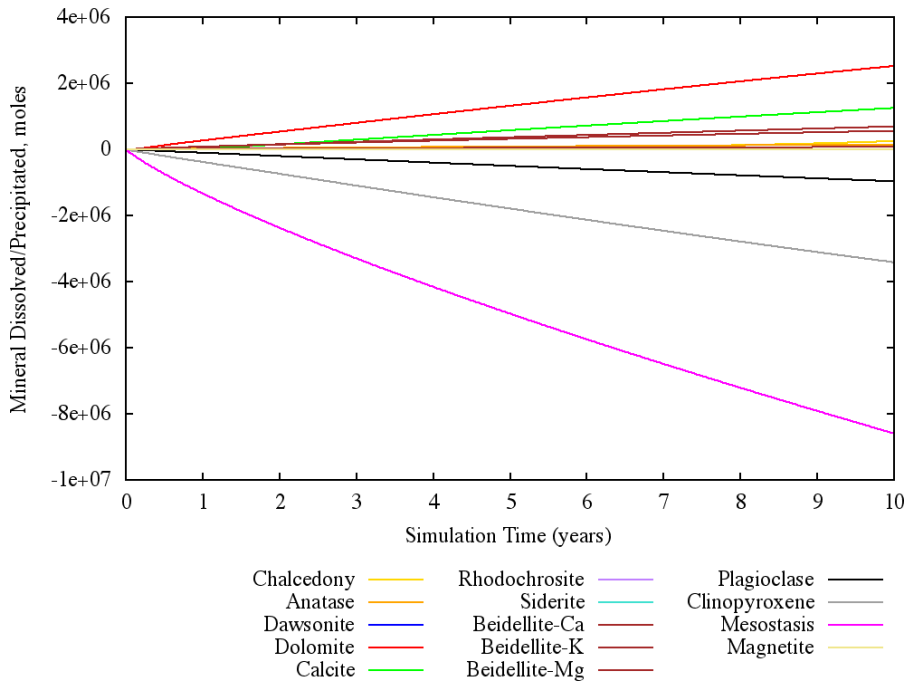


Figure 4. Change in mineral mass (total moles in model domain, negative value indicates dissolution, positive value indicates precipitation) after 1000 MT of CO₂ Injection into the Slack Canyon #2 Flow Top

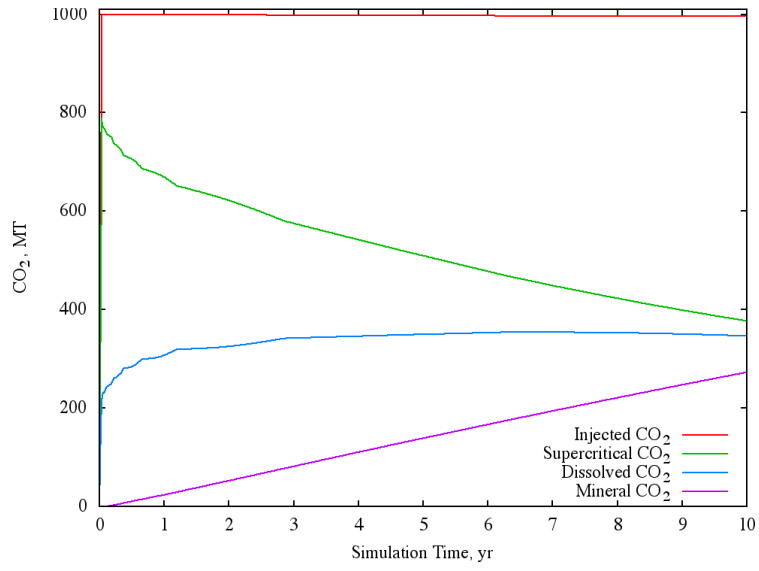


Figure 5. Mass balance of 1000 MT of CO₂ Injection into the Slack Canyon #2 Flow Top

Exercises

1. Set the glass reaction rate to zero. Rerun the simulation. Compare the amount of mineral sequestration relative to the base case simulation. Plot the porosity at the end of the injection period and at the end of 10 years. Does the porosity increase or decrease? Compare the densities of the dissolving and precipitating minerals.

References

- Bacon DH and EM Murphy. 2011. "Managing Chemistry Underground: Is Co-Sequestration an Option in Selected Formations?" *Energy Procedia*, 4:4457-4464.
- Gunter WD, B Wiwchar, and EH Perkins. 1997. "Aquifer disposal of CO₂-rich greenhouse gases: Extension of the time scale of experiment for CO₂-sequestering reactions by geochemical modelling." *Mineralogy and Petrology*, 59(1-2):121-140.
- McGrail BP, FA Spane, EC Sullivan, DH Bacon, and G Hund. 2011. "The Wallula Basalt Sequestration Pilot Project." *10th International Conference on Greenhouse Gas Control Technologies*, 4:5653-5660.
- McGrail BP, EC Sullivan, PD Thorne, FA Spane, Jr., CJ Thompson, DH Bacon, SP Reidel, G Hund, and FS Colwell. 2009. *Preliminary Hydrogeologic Characterization Results from the Wallula Basalt Pilot Study*. PNWD-4129, Battelle, Pacific Northwest Division, Richland, Washington.
- Palandri JL and YK Kharaka. 2004. *A Compilation of Rate Parameters of Water-Mineral Interaction Kinetics for Application to Geochemical Modeling*. Open File Report 2004-1068, U.S. Geological Survey, Menlo Park, California.
- Schaef HT, BP McGrail, and AT Owen. 2010. "Carbonate mineralization of volcanic province basalts." *International Journal of Greenhouse Gas Control*, 4(2):249-261.
- Strait SR and FA Spane, Jr. 1982. *Preliminary results of hydrologic testing the composite Umtanum basalt flow top at borehole RRL-2*. SD-BWI-TI-105, Rev. 0, Rockwell Hanford Operations, Richland, Washington.
- White MD, BP McGrail, HT Schaef, and DH Bacon. 2006. "Numerically simulating carbonate mineralization of basalt with injection of carbon dioxide into deep saline formations." *CMWR XVI - Computational Methods in Water Resources XVI International Conference*, Copenhagen, Denmark.
- Wolery TW and RL Jarek. 2003. *Software User's Manual, EQ3/6, Version 8.0*. Sandia National Laboratories, Albuquerque, New Mexico.
- Xu TF, JA Apps, and K Pruess. 2005. "Mineral sequestration of carbon dioxide in a sandstone-shale system." *Chemical Geology*, 217:295-318.